




Circadian networks in human embryonic stem cell-derived cardiomyocytes

Pieterjan Dierickx^{1,2,3,*} , Marit W Vermunt¹, Mauro J Muraro¹, Menno P Creyghton¹, Pieter A Doevendans^{2,4}, Alexander van Oudenaarden¹, Niels Geijsen^{1,†}  & Linda W Van Laake^{2,3,†,**} 

Abstract

Cell-autonomous circadian oscillations strongly influence tissue physiology and pathophysiology of peripheral organs including the heart, in which the circadian clock is known to determine cardiac metabolism and the outcome of for instance ischemic stress. Human pluripotent stem cells represent a powerful tool to study developmental processes *in vitro*, but the extent to which human embryonic stem (ES) cell-derived cardiomyocytes establish circadian rhythmicity in the absence of a systemic context is unknown. Here we demonstrate that while undifferentiated human ES cells do not possess an intrinsic functional clock, oscillatory expression of known core clock genes emerges spontaneously during directed cardiac differentiation. We identify a set of clock-controlled output genes that contain an oscillatory network of stress-related transcripts. Furthermore, we demonstrate that this network results in a time-dependent functional response to doxorubicin, a frequently used anti-cancer drug with known cardiotoxic side effects. Taken together, our data provide a framework from which the effect of oscillatory gene expression on cardiomyocyte physiology can be modeled *in vitro*, and demonstrate the influence of a functional clock on experimental outcome.

Keywords cardiomyocytes; circadian rhythms; human embryonic stem cells

Subject Categories Development & Differentiation; Stem Cells

DOI 10.15252/embr.201743897 | Received 3 January 2017 | Revised 29 March 2017 | Accepted 10 April 2017 | Published online 23 May 2017

EMBO Reports (2017) 18: 1199–1212

Introduction

The circadian clock is a conserved time-keeping system that regulates numerous body features such as behavior, metabolism, body temperature, tissue regeneration, and organ homeostasis in a diurnal manner [1]. In the heart, the role of 24-h rhythmicity is illustrated by oscillations in heart rate, blood pressure, and cardiac

output [2–6]. The circadian clock comprises a central clock in the brain (the suprachiasmatic nucleus (SCN)) and peripheral clocks that are present in almost all organs. The SCN is mainly entrained by light and subsequently synchronizes the peripheral clocks via neural and humoral factors [7]. Interestingly, peripheral clocks function in a cell-autonomous manner. When ablating the SCN, these clocks remain functional and even synchronized when subjected to a restricted feeding regime [8,9]. Autonomous rhythmicity is underscored by the persistence of circadian rhythms in *in vitro* cultured cells.

The molecular mechanism that underlies the core clock machinery consists of a transcriptional/translational feedback loop in which a heterodimer of BMAL1 and CLOCK drives rhythmic transcription of downstream genes. These include other core clock genes (period 1 (*PER1*), *PER2*, *PER3*, cryptochrome 1 (*CRY1*), *CRY2*, *ROR α / β* , *REV-ERB α / β*) as well as clock-controlled genes (CCGs) that determine circadian organ physiology in a tissue-specific manner. In the murine heart, ~6–12% of the expressed genes have a circadian expression pattern [10–14]. Rhythmicity is essential for human tissue homeostasis as well, as highlighted by the fact that genetic or environmental (e.g., shift-work) perturbation of the circadian clock results in a vast array of malignancies such as sleep disorders, inflammation, cancer [15], impairment of regenerative capacity [16,17], metabolic disorders [18–20], and cardiovascular diseases [13,21–24]. In addition, the onset of multiple malicious cardiac events is known to follow a diurnal pattern. Myocardial infarction [25,26], arrhythmias [27,28], and sudden cardiac death [29,30] show a higher incidence in the sleep-to-wake transition in humans. The important role of circadian rhythmicity in cardiac injury and regeneration is further solidified by genetic experiments in mice in which a cardiomyocyte-specific mutation of the *Clock* gene has been shown to blunt the heart's response to induced ischemic damage [31]. Accordingly, clinical studies revealed that infarcts were larger and led to increased reduction in cardiac function when occurring in the sleep-to-wake transition [32–34].

Human pluripotent stem cell-derived cardiomyocytes have emerged as a potential cellular source for replacement therapies. In

1 Hubrecht Institute-KNAW and University Medical Center Utrecht, Utrecht, The Netherlands

2 Division of Heart and Lungs, Department of Cardiology, University Medical Center Utrecht, Utrecht, The Netherlands

3 Regenerative Medicine Center Utrecht, University Medical Center Utrecht, Utrecht, The Netherlands

4 Netherlands Heart Institute, Utrecht, The Netherlands

*Corresponding author. Tel: +31 302121800; E-mail: p.dierickx@hubrecht.eu

**Corresponding author. Tel: +31 887555555; E-mail: l.w.vanlaake@umcutrecht.nl

†These authors contributed equally to this work

addition, human ES cell-derived as well as induced pluripotent stem cell-derived cardiomyocytes are increasingly used for disease modeling and drug testing [35]. While circadian rhythms play an essential role in cardiomyocyte function *in vivo*, nothing is known about circadian control of gene expression in pluripotent stem cell-derived cardiomyocytes, which are often used to model cardiac function and disease.

Here we analyze temporal clock gene expression networks in human ES cells and ES cell-derived cardiomyocytes. We demonstrate that circadian rhythmicity is absent in human ES cells and is established progressively during directed cardiac differentiation. The identified oscillatory networks are shown to significantly influence the function of human ES cell-derived cardiomyocytes and determine their response to externally applied stressors. Our findings underscore that circadian rhythmicity can affect experimental outcome, which may have important ramifications for processes such as timed cell-based therapy.

Results

Human embryonic stem cells express clock genes in a non-oscillatory manner

Nearly all cells in the human body possess a functional clock as indicated by circadian rhythmicity of core clock gene expression. However, whether human embryonic stem (ES) cells display a functional circadian clock is unknown. Therefore, we compared global expression levels of six core clock genes *ARNTL* (coding for and henceforth referred to as *BMAL1*), *PER2*, *CRY1*, *CRY2*, *CLOCK*, and *NR1D1* between pluripotent human ES cells and differentiated human osteosarcoma U2OS cells, a cell line known to possess a functional clock as confirmed here by anti-phasic *Bmal1*-dLuc and *Per2*-dLuc signal after transduction of promoter-based lentiviral luciferase constructs [36,37] (Fig 1A and B). Transcripts of all genes could be detected in both cell types, with five out of six core clock genes having higher expression levels in U2OS cells compared to human ES cells (Student's *t*-test, $P < 0.05$; Fig 1C). Only *CRY1* showed a trend toward higher expression in human ES cells (Student's *t*-test, $P = 0.0506$; Fig 1C), which is in line with previously reported observations in mouse ES and NIH3T3 cells [38]. Protein levels of *BMAL1*, *CRY1*, and *CLOCK* were detected by Western blot (Fig 1D, left and Fig EV1) at corresponding levels to their mRNA transcripts (Fig 1D, right). From this, we conclude that while core clock genes are expressed and translated into proteins in human ES cells, this occurs with a different stoichiometry in comparison with U2OS cells and most likely also other differentiated cell types.

The presence of core clock proteins in human ES cells led us to investigate their possible rhythmic expression over time. To this end, human ES cells were synchronized with forskolin [39], and *BMAL1* and *PER2* mRNA levels were measured every 4 h over a period of 48 h using qRT-PCR. Significance of 24-h rhythmicity was assessed using RAIN, a nonparametric method detecting arbitrary wave forms in biological data [40]. No apparent oscillatory expression pattern could be identified over the course of 2 days (RAIN, *BMAL1*, $P > 0.99$ and *PER2*, $P = 0.97$; Fig 1E). Additionally, to assess *BMAL1* and *PER2* transcription over time in human ES cells, we transduced human ES cells with *Bmal1*- and

Per2-promoter-based lentiviral luciferase constructs [36,37]. After synchronization, no rhythmic bioluminescence was observed (Fig 1F). Therefore, clock genes are expressed in human ES cells, but in a non-circadian manner.

Human embryonic stem cell differentiation toward cardiomyocytes

Multi-lineage differentiation of human ES cells has proven extremely valuable to understand developmental processes as well as to provide clinically relevant populations for cell-based therapy and drug testing [41]. To assess the presence of a functional clock upon differentiation, circadian rhythmicity was analyzed at two additional stages (D15 and D30) during directed differentiation of human ES cells toward cardiomyocytes (Fig 2A). To allow for the identification of early cardiac cells, we made use of a *NKX2-5*-eGFP (Homeobox protein *NKX2-5*-eGFP) reporter human ES cell line [42]. Cardiac differentiation of human ES cells typically yields significant contribution of cardiomyocytes to the total population of cells [43–45], which was also seen here with ~50% cardiomyocytes around D15 as defined by FACS for cTNNT2 (cardiac Troponin T) (Fig EV2A). Different stages were characterized by clear changes in marker gene expression (Fig 2A). At day 0 (D0), cells expressed the pluripotency markers *NANOG* and *POU5F1*, both at the mRNA and protein level (Figs 2A and B, and EV2B). Upon differentiation, pluripotency factors quickly decreased and the expression of cardiac markers, such as *NKX2-5* and *ACTC1* (actin alpha cardiac muscle 1), was observed in both (D15 and D30) spontaneously beating cultures as measured by qRT-PCR (Fig 2A). Immunostainings for α -sarcomeric ACTIN and cTNNT2 confirmed sarcomeric structures at D15 and D30 (Fig 2B). Additionally, staining for MEF2C (Myocyte Enhancer Factor 2C) and GFP, to assess the presence of *NKX2-5*-eGFP-positive cells, revealed the abundance of cardiomyocytes at D15 and D30. While the early cardiomyocyte progenitor marker *ISL1* (insulin gene enhancer protein ISL-1) was highly expressed at D15, maturation markers such as *KCNJ2* (inward rectifier potassium channel 2) and *SERCA2A* (sarcolemmal/endoplasmic reticulum Ca^{2+} ATPase) [44,46] were the highest at D30 (Fig 2A). These results validate the *in vitro* transcriptomic maturation of these cells between D15 and D30, and confirm that the different stages represent distinct cardiac states that can be used to assess the presence of a functional clock across the transition from human ES cells to cardiomyocytes.

Rhythmic expression of clock genes emerges during cardiac differentiation

Whether and when human ES cells develop a functional clock upon differentiation, in the absence of systemic cues, is unknown. To investigate the possibility of an emerging clock, we compared mRNA levels of *BMAL1*, *PER2*, and *CLOCK* in D0 human ES cells and D15 and D30 human ES cell-derived cardiac cells. Even though *BMAL1*, *PER2*, and *CLOCK* were expressed at all stages, their expression increased significantly from D0 to D15 and/or D30 (ANOVA with Bonferroni correction, $P < 0.05$; Fig 3A). This indicates that core clock gene expression levels gradually increase during directed cardiac differentiation.

To assess rhythmicity of clock gene expression at D15 and D30, cells were synchronized using dexamethasone [47] and three

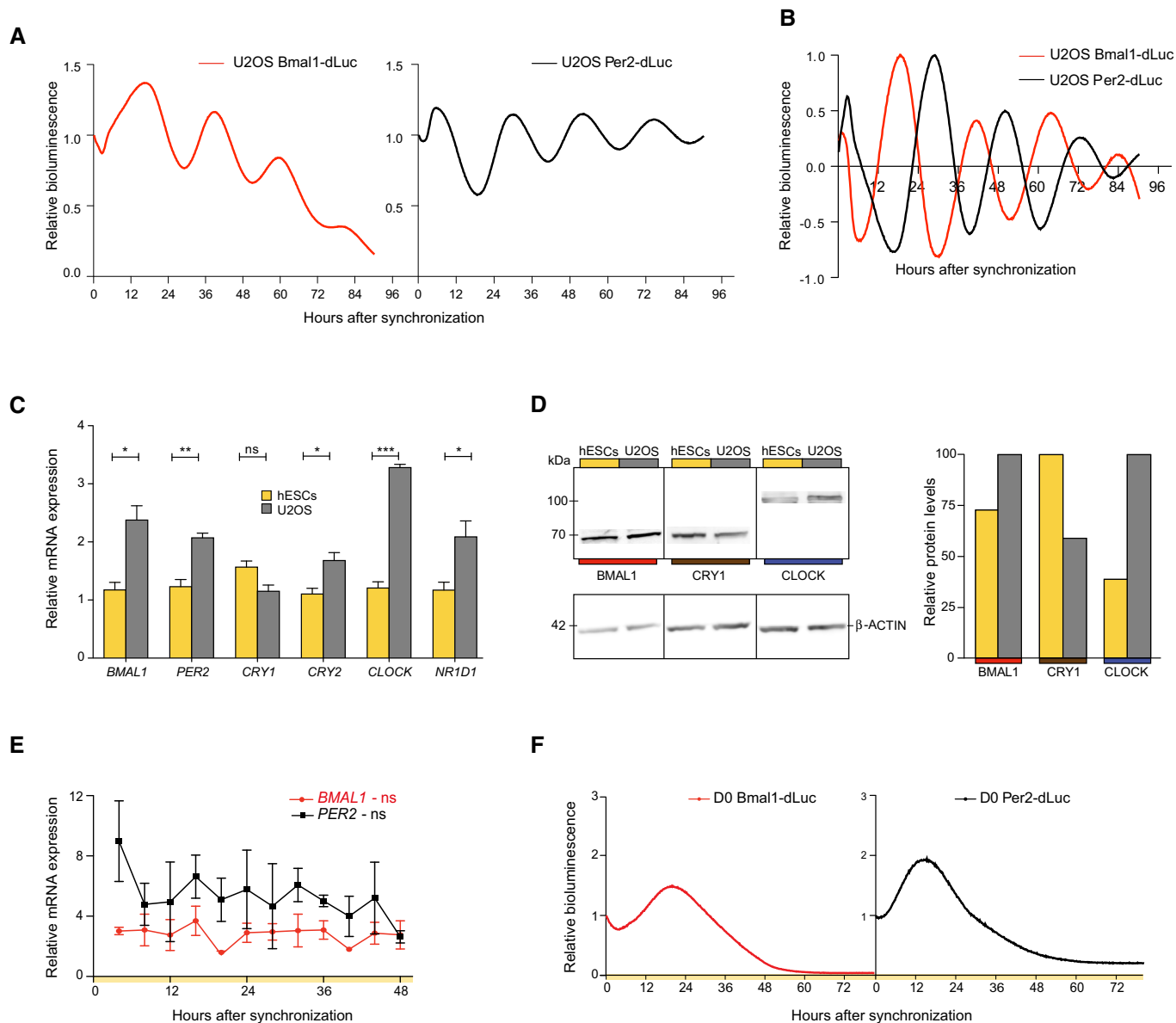


Figure 1. Non-oscillatory expression of clock genes in human ES cells.

A Raw lentiviral promoter-based luciferase reporter bioluminescence in U2OS cells after dexamethasone synchronization. Bioluminescence was measured with a LumiCycle32. Values are relative to T0.
 B Detrended bioluminescent signals measured in (A).
 C *BMAL1*, *PER2*, *CRY1*, *CRY2*, *CLOCK*, and *NR1D1* expression levels in human ES cells compared to U2OS cells as determined by qRT-PCR. Expression levels were normalized to *PPIA* and compared between cell types using an unpaired two-tailed Student's *t*-test (ns: not significant, **P* < 0.05, ***P* < 0.005, and ****P* < 0.0005). Data are represented as mean ± s.e.m. of three independent replicates.
 D Western blot for *BMAL1*, *CRY1*, and *CLOCK*. Protein levels were quantified and normalized to β-ACTIN.
 E qRT-PCR analysis of *BMAL1* and *PER2* expression over 48 h at a 4-h interval in human ES cells. Circadian oscillations were analyzed using the RAIN algorithm, and the significance of rhythmicity across 48 h is indicated (ns: not significant). Data are represented as mean ± s.e.m. of three independent replicates.
 F *Bmal1*-dLuc and *Per2*-dLuc values in synchronized human ES cells across 76 h measured by LumiCycle32. Representative tracks are shown. Values are relative to T0.

independent RNA samples were collected every 4 h over a period of 48 h (Fig EV3). *BMAL1* and *PER2* levels were analyzed by qRT-PCR to determine whether their expression oscillated in an anti-phasic manner, a hallmark of a functional molecular circadian clock. Similar to undifferentiated human ES cells (Fig 1E), no clear circadian pattern was observed in the early stage D15 human ES cell-derived

cardiomyocytes (D15; RAIN, *P* = 0.095, *P* = 0.68 for *BMAL1* and *PER2*, respectively; Fig 3B). Matured cardiac cells, however, showed significant oscillations for *PER2* but not *BMAL1* (D30; RAIN, *P* = 1.4E-8 and *P* = 0.81; Fig 3B). To further validate the emergence of a functional clock, cultures were transduced with *Bmal1*-dLuc and *Per2*-dLuc lentiviral reporters. At D15, after synchronization, a

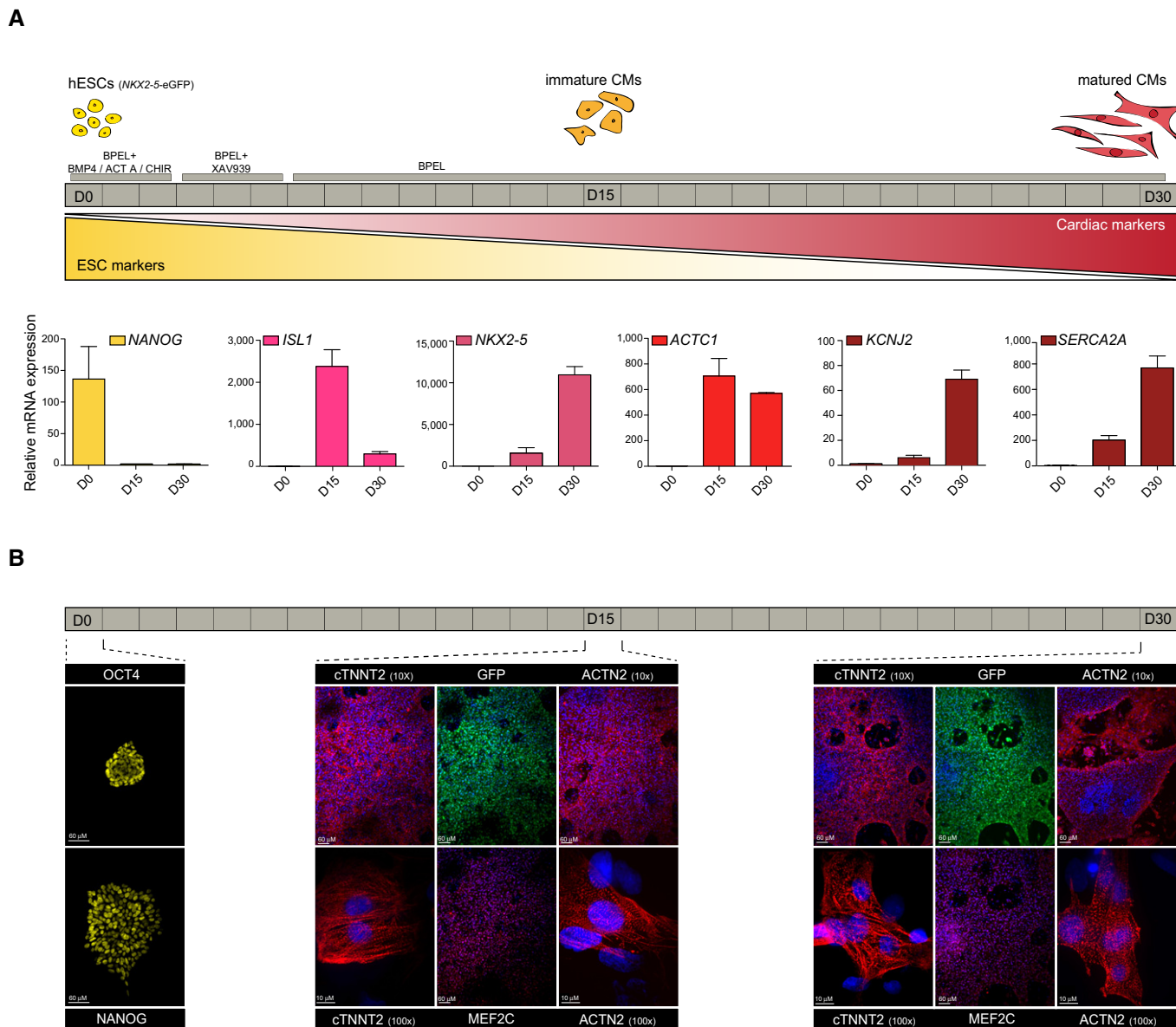


Figure 2. Characterization of distinct stages of cardiac differentiation.

A Schematic of the directed cardiac differentiation and the three different stages used in this study. hESCs: human embryonic stem cells. CM: cardiomyocyte. Below are mRNA expression levels of pluripotency and cardiac markers as measured by qRT-PCR. Expression levels were normalized to a non-oscillatory housekeeping gene (*PPIA*). Data are represented as mean \pm s.e.m. of three independent replicates.

B Immunostaining for pluripotency markers OCT4 and NANOG (yellow) in human ES cells. cTNNT2 and sarcomeric actin (red) stainings reveal clear sarcomeric structures at all cardiac stages. Cardiomyocyte nuclei were stained for MEF2C (red), *NKX2-5-eGFP*-positive cells were stained with anti-GFP (green) and nuclei with Hoechst (blue).

small induction of oscillatory *Per2*-based luciferase signal could be detected (Fig 3C), which is in line with previously described observations of *Per2* as an early oscillator upon retinoic acid induced differentiation in mouse ES cells [48]. In D30 synchronized populations, typical anti-phasic oscillatory *Per2*- and *Bmal1*-driven bioluminescence levels were observed, which confirms the presence of a clock at D30 (Figs 3D and E, and EV4A and B).

In order to verify the contribution of cardiomyocytes to the observed oscillatory pattern in our cardiac cultures, *NKX2-5-eGFP*⁺

cells were purified via FACS. After sorting, strong *Bmal1*-dLuc and *Per2*-dLuc rhythmicity was detected in synchronized human ES cell-derived cardiomyocytes (Figs 3F and EV4C and D). In addition to these observations in a sorted population, circadian *Per2*-dLuc patterns were also found in bioluminescence recordings of single *NKX2-5-eGFP*⁺ human ES-derived cardiomyocytes (Figs 3G and H, and EV4D), which further confirms the presence of a functional clock in D30 cardiomyocytes. To question whether circadian rhythmicity would persist during culture, 45 days old cardiac cultures

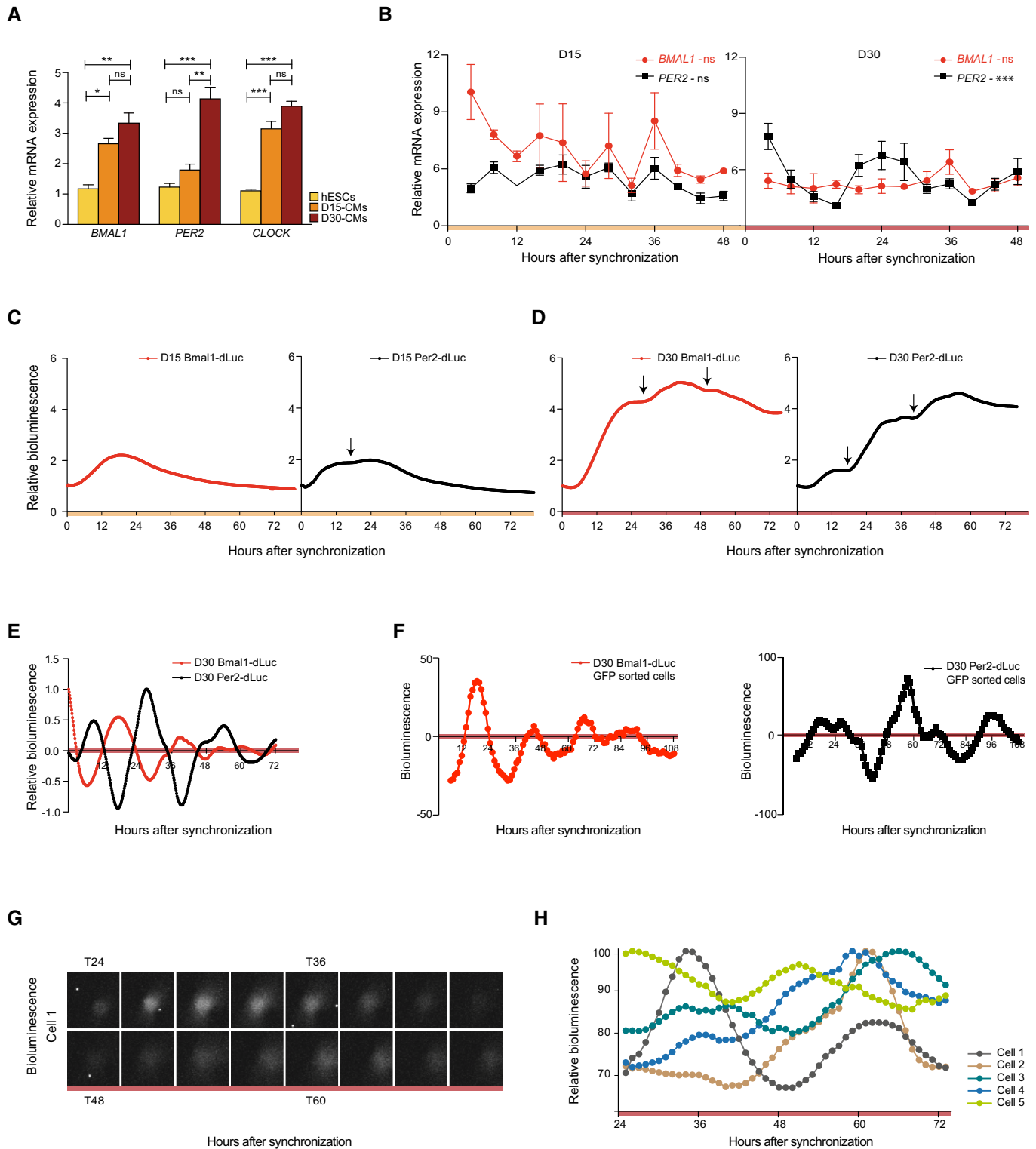


Figure 3.

were analyzed using real-time reporter-based luciferase measurements. Significant Per2- and Bmal1-dLuc oscillations were observed (Fig EV4E). These results indicate that human ES cells develop a functional clock upon directed cardiac differentiation, with robust oscillations at D30 that persist in older *in vitro* cultures.

Human ES cell-derived cardiomyocytes show a network of stress-related clock output genes

A functional circadian clock translates into the oscillatory expression of clock-controlled genes (CCGs). Gene expression profiling in

Figure 3. Rhythmic clock gene expression emerges in (matured) cardiac cultures.

- A *BMAL1*, *PER2*, and *CLOCK* expression levels at D0, D15, and D30 during directed cardiac differentiation as determined using qRT-PCR. Data are represented as mean \pm s.e.m. of three independent replicates. Significant expression differences were tested by one-way ANOVA, followed by a Bonferroni *post hoc* test (ns: not significant, * $P < 0.05$, ** $P < 0.005$, *** $P < 0.0005$).
- B qRT-PCR analysis of *BMAL1* and *PER2* expression over 48 h at a 4-h interval in cardiac cells at D15. Expression levels in (A) and (B) were normalized to *PP1A*. Data are represented as mean \pm s.e.m. of three independent replicates. Significance of rhythmicity across 48 h was analyzed using the RAIN algorithm and is indicated (ns: not significant, *** $P < 0.0005$).
- C Promoter-based destabilized luciferase (dLuc) reporter assay of the *Bmal1* and *Per2* promoter in synchronized cardiac cells at D15. Values are relative to T0. Measurements were performed using a LumiCycle32.
- D Similar analysis as in (C) for D30.
- E Detrended *Bmal1*-dLuc and *Per2*-dLuc luciferase signal measured in (D).
- F Detrended *Bmal1*-dLuc and *Per2*-dLuc bioluminescence in *NKX2-5*-eGFP⁺ sorted and synchronized human ES cell-derived cardiomyocytes at D30.
- G Single-cell analysis of *Per2*-dLuc bioluminescence in sorted eGFP-positive and synchronized D30 human ES cell-derived cardiomyocytes.
- H Representative *Per2*-dLuc signal in five single D30 human ES cell-derived cardiomyocytes over the course of 48 h.
- Data information: Measurements in (F–H) were performed with a LV200 microscope.

numerous cell types and tissues has shown that around 3–16% of the transcriptome exhibits circadian rhythmicity [14]. Conform differing physiological demands of organs, oscillating output genes vary per tissue. For the murine heart, ~6–12% of the expressed genes were shown to oscillate in a 24-h manner [10–14]. To identify CCGs during *in vitro* cardiomyocyte differentiation, genome-wide mRNA levels were assessed by mRNA sequencing of purified RNA using CEL-Seq, a previously described RNA profiling technique based on sequencing the 3'UTR of mRNAs, generating one read per transcript [49]. We first compared the overall transcriptional profile of matured cardiac cells (D30) to that of human ES cells and D15 cultures 48 h post-synchronization (Fig EV5A and Table EV1). Lowly expressed genes are typically not picked up robustly when analyzing highly multiplexed CEL-Seq data at relatively low sequencing depth. To control for this, genes with an average of < 3 RPM (reads per million) across all time points were not used for further analysis. Based on ~14,000 genes with an expression level of more than 3 RPM at one of the stages, Spearman's rank correlation coefficients (ρ) showed that transcriptional programs were substantially different between cardiac cells at D15 and D30 ($\rho = 0.53$; Fig EV5A–C). Observed changes between states were consistent between our qRT-PCR and CEL-Seq analyses, as indicated for several marker genes, which highlights the reliability of our sequencing datasets (Figs 2A and EV5D). Indeed, increased *MYH7*/*MYH6* levels and multiple other markers (e.g., *MYL2*, *PLN*, and *KCNJ2*) confirm *in vitro* cardiomyocyte maturation as well as generally higher clock gene expression across differentiation (Fig EV5C and D).

To assess the possible presence of oscillatory transcripts at D15 and the identity of CCGs in D30 cardiac cells, in which a functional clock was found (Fig 3), three independent RNA samples were collected every 4 h over a period of 48 h and sequenced using CEL-Seq (Fig EV3 and Table EV1). Around 10,000 genes had an average expression of more than 3 RPM in both D15 and D30 (Fig EV3) and were screened for oscillatory expression over 48 h as determined by JTK-cycle [50]. This revealed 643 and 757 oscillating transcripts ($P < 0.05$) at D15 and D30, respectively (Fig 4A and Table EV2). The oscillatory transcripts of D15 could result from a starting clock as indicated by small circadian *Per2*-dLuc signals at this time point (Fig 3C), but are mostly distinct from the CCGs that were found at D30 (Fig 4B). This limited fraction of overlap might be an underrepresentation, as detecting oscillatory transcription of genes has been

shown to rely strongly on sequencing depth [51]. Relatively low expression also explains the absence of core clock genes from the rhythmic transcripts (Fig EV5D). Indeed, in our data for both D15 and D30, oscillatory genes had on average more coverage than non-oscillatory transcripts (Fig EV5E) and shared oscillators between D15 and D30 ($n = 80$) had higher expression levels than stage-specific oscillators (Fig EV5F). A fraction of the oscillators (D15 only, D30 only and shared) was found to overlap known mouse cardiac CCGs [14] (Fig 4C) including genes with a known important role in cardiomyocytes (*COL4A1*, *SPON2*, *SLC23A2*, *AQP1*, and *STC1*; Fig 4D) [52–55]. These data thus contain common rhythmically expressed clock-controlled genes between mouse hearts and human ES cell-derived cardiomyocytes.

STRING protein–protein analysis [56] on D30 oscillators that were also found to have circadian expression in mouse hearts ($n = 135$; Table EV2) revealed a putative, highly interactive network (Fig 5A). D15 rhythmic transcripts that overlap mouse heart oscillators ($n = 98$), however, did not show such interactions (Fig 5B). Gene ontology (GO) analysis for these oscillators showed enrichment for extracellular matrix formation terms at D15, while D30 oscillators were enriched for cardiac development and stress response terms (Fig 5A and B). Interestingly, the D30 interaction network was centered around *UBC* (ubiquitin C) (Fig 5A), one of the four genes encoding for ubiquitin in mammals and one of the most abundant proteins in eukaryotic cells [57]. Although *Ubc* is expressed in multiple tissues in mice (<http://biogps.org/>) [58], it has only been shown to oscillate in the murine heart [52] and (skeletal) muscle [14] (JTK, $P = 3.32E-6$ and $P = 5.97E-7$, respectively; Fig 5C). This suggests that *Ubc* is a heart- and muscle-specific CCG *in vivo*, and concurs with our identification of *UBC* as a circadian CCG in *in vitro* D30 human ES cell-derived cardiomyocytes (D30, JTK, $P = 0.0032$; Fig 5D). Among the putative *UBC* interacting partners, several genes were known oscillators in the murine heart according to the CircaDB database (<http://circadb.hogeneschlab.org/>) [11,14,59]. Interestingly, many of the oscillating *UBC* interaction partners in D30 human ES cell-derived cardiomyocytes were involved in cardiac function (*PLN*) [60], stress response (*BNIP3*, *RRAGA*, *DNAJA1* and *HSPH1*) [61], hypertrophy (*RGS2*) [62], and even contained therapeutic targets such as *TSPO* (Translocator protein) [63] (Fig 5D). This indicates that the oscillators that were identified here possibly contribute to multiple molecular mechanisms with a circadian clock dependency, but could also suggest a

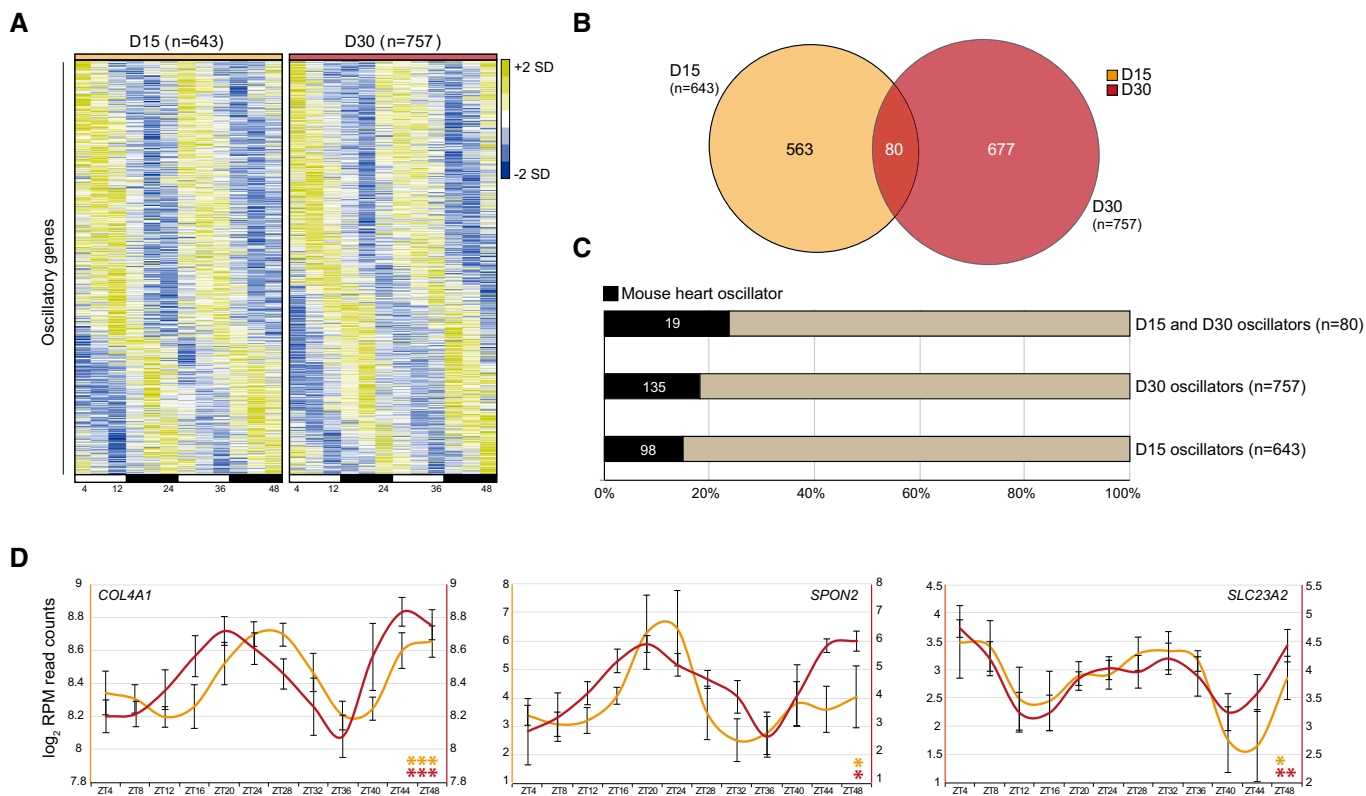


Figure 4. Identification of oscillatory transcripts at D15 and D30.

- A 643 and 757 oscillators for D15 and D30 cultures, as analyzed using JTK-cycle (adj. $P < 0.05$). Heatmaps represent z-normalized RPM values of the average of three independent replicates. Oscillatory genes were ranked by their phase of expression and visualized using Java TreeView.
- B Venn diagram of JTK-cycle detected oscillators for D15 and D30.
- C Fraction of JTK-cycle detected oscillators that were previously found to be rhythmically expressed in mouse hearts [14].
- D Examples of overlapping oscillators between D15, D30 cardiac cells and mouse hearts. Average \log_2 RPM read counts of three replicates, smoothed over 2 time points \pm s.e.m., were plotted. Significance of rhythmicity across 48 h was analyzed using the JTK-cycle algorithm (* JTK $P < 0.05$, ** JTK $P < 0.005$, and *** JTK $P < 0.0005$).

role for circadian processes in pathophysiological events such as ischemic damage after myocardial infarction.

Human ES cell-derived cardiomyocytes show rhythmicity in doxorubicin-induced apoptosis

Mouse hearts show circadian rhythmicity in their tolerance to ischemia and reperfusion after myocardial infarction [31]. In

humans, a similar time of the day pattern in the onset and severity of myocardial infarction has been described [25,32–34,64,65]. The combination of time-dependent pathophysiology and the enrichment of oscillating stress-associated genes (around *UBC*) in our CEL-Seq datasets prompted us to assess whether *in vitro* derived cardiac cells would show a functional circadian reaction to induced stress. The anthracycline doxorubicin is a widely used anti-cancer drug that is often administered in the clinic, but is also known to have severe

Figure 5. Circadian stress network results in time-dependent apoptotic response of human ES cell-derived cardiac cultures.

- A STRING interaction network of overlapping oscillators between D30 cardiac cells and mouse hearts with corresponding GO analysis. Genes that oscillate at both D15 and D30 are depicted in pink. Mouse heart oscillators were deduced from Zhang et al [14].
- B Same analysis as in (A) for D15 oscillators.
- C *Ubc* mRNA oscillation in mouse hearts and skeletal muscle. Data were obtained from CircaDB (<http://circadb.hogenschlab.org/>, deduced from [14,83]). Corresponding CircaDB P -values are indicated.
- D Expression levels of four D30 oscillatory genes (*UBC*, *RGS2*, *PLN*, and *TSPO*) across 48 h. Average \log_2 RPM CEL-Seq counts of three replicates were plotted for D15 and D30 and smoothed over two time points \pm s.e.m. Significance of rhythmicity across 48 h was analyzed using the JTK-cycle algorithm (ns: not significant; * JTK $P < 0.05$, ** JTK $P < 0.005$, and *** JTK $P < 0.0005$).
- E Apoptosis, as measured by caspase 3/7 activity, after doxorubicin administration in D15 and D30 human ES cell-derived cardiac cells across all samples from (F) and (G). Bottom and top of the boxes are the 25th and 75th percentiles. The line within the boxes represents the median and whiskers denote the minimum and maximum values. The effect of doxorubicin versus DMSO was tested using a Mann–Whitney U -test (*** $P < 0.0005$).
- F Apoptosis measured with 6-h intervals in synchronized D15 cultures after administration of doxorubicin (orange) and DMSO as control (black) for 6 h. Data are represented as the mean \pm s.e.m. of three independent replicates. Significance of rhythmicity across 48 h was analyzed using the RAIN algorithm and is indicated (ns: not significant).
- G Same as in (F) for D30 cultures with the doxorubicin response depicted in red (RAIN, ns: not significant and * $P < 0.05$). Data are represented as the mean \pm s.e.m. of three independent replicates.

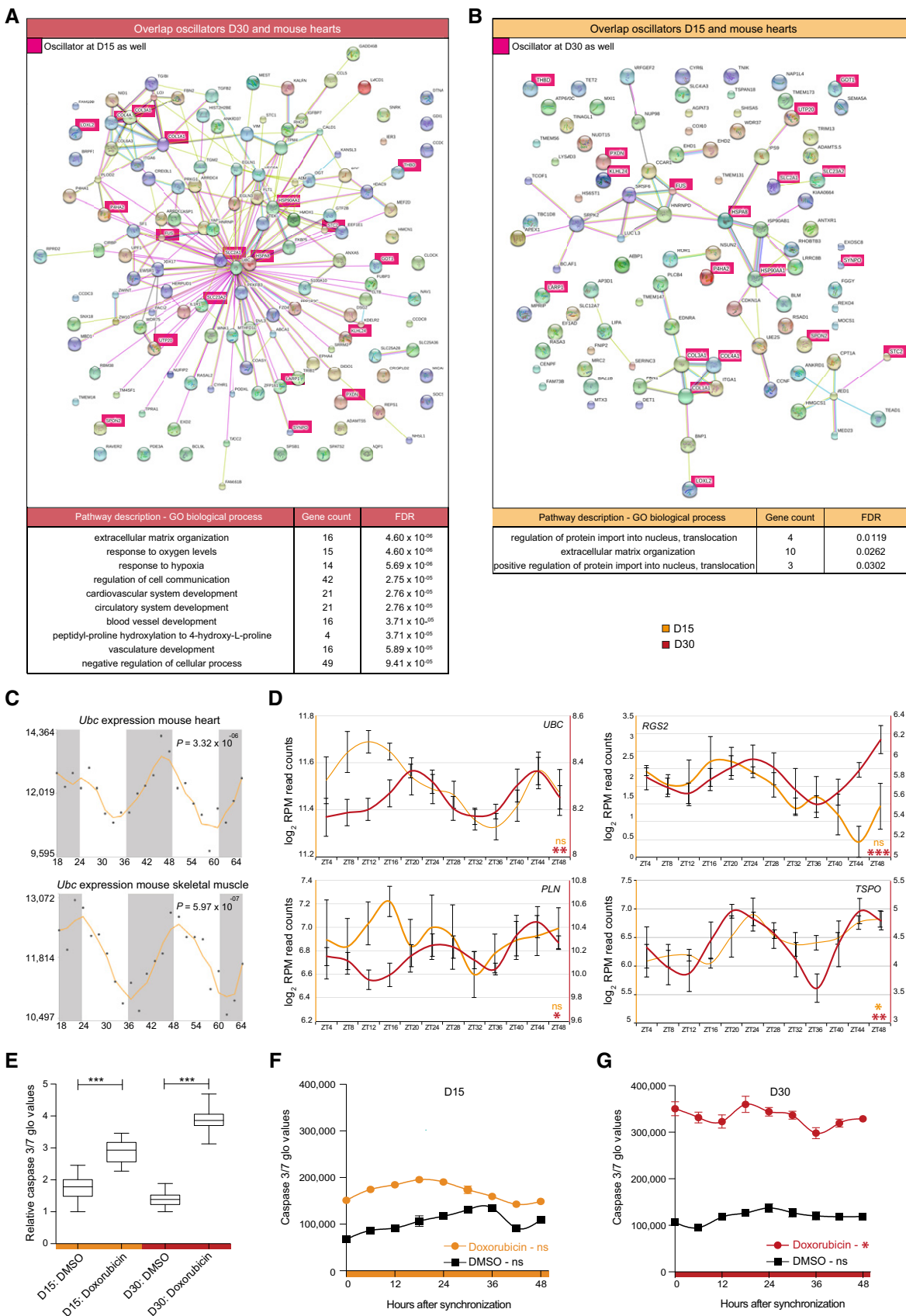


Figure 5.

cardiotoxic side effects [66,67]. These effects are recapitulated in *in vitro* human ES cell-derived cardiomyocytes in which doxorubicin is known to induce apoptosis and has proven to be a good model for induced cardiotoxicity [68,69]. To determine whether the sensitivity of human ES cell-derived cardiac cells to doxorubicin-induced apoptosis displays an oscillatory response, we synchronized cultures at D15 and D30 and administered doxorubicin (10 μ M) every 6 h over the course of 48 h (see Materials and Methods). A marked induction of apoptosis was found at both stages, as indicated by elevated active caspase 3/7 levels over control DMSO-treated samples (Mann–Whitney *U*-test, $P < 0.0005$ for D15 and D30; Fig 5E), with matured D30 cells being more sensitive to doxorubicin than D15 cultures ($P < 0.05$). Interestingly, the strength of the apoptotic response demonstrated a significant circadian pattern at D30, but not D15 (RAIN, $P < 0.05$ and $P = 0.85$ for D30 and D15, respectively; Fig 5F and G), which reveals the functional consequences of a circadian clock in cardiomyocytes. These results highlight the potential of reducing cardiotoxic side effects by the use of time-based cancer therapy, but also indicate that taking diurnal rhythmicity into account could possibly improve other treatment strategies.

Discussion

Circadian rhythmicity is crucial to heart function, but also influences pathophysiology as indicated by, for instance, diurnal rhythmicity of cardiac damage after infarction [25,31–34,64,65]. As human ES cell-derived cardiomyocytes are emerging as a powerful tool to model developmental and disease processes as well as being a potential cellular source for regenerative therapies, we examined the presence and possible implications of a functional clock in human ES cells and their cardiac derivatives. While human ES cells do express core clock genes, no circadian clock was observed. Upon differentiation toward cardiomyocytes however, a functional core clock pathway was gradually

established (Fig 6) as determined by robust anti-phasic oscillations of *BMAL1* and *PER2*. This work is the first demonstration of a functional clock in human ES cell-derived (cardiac) cells and may serve as a paradigm for the emergence of diurnal rhythms in other human pluripotent stem cell-derived cell types. At D30, 757 CCGs were identified, 18% of which are known to oscillate in the murine heart. Importantly, our data uncover additional transcripts with specific oscillatory behavior in human ES cell-derived cardiomyocytes. As some of these newly identified oscillators are known to play an important role in human heart physiology (*PLN*, *KCNE4*, *TSPO*, *CAV1*, *RGS2*), this stresses the importance of using human cells for modeling cardiovascular processes and disease.

Importantly, a defined set of the oscillators could clearly be linked to stress response, which was confirmed by a time-dependent response to doxorubicin administration. This highlights the possible beneficial effects of drug administration at a specific time of the day to decrease cardiotoxic side effects. Notably, next to explicit clock synchronization steps, such as with forskolin or dexamethasone, simple medium changes can also reset the internal clock of cell cultures [70]. Our results demonstrate that circadian mechanisms can influence cellular response to external stressors and thus is an important factor to consider when interpreting experimental results. Our data stress the importance of testing compounds in a time-controlled manner when using *in vitro* cultured cardiomyocytes, and may also extend to other ES cell-based disease models.

Materials and Methods

ESC culture and cardiomyocyte differentiation

NKX2-5-eGFP human ES cells [42] (stable reporter line generated from wild-type HES3 cells [71]) were cultured in Essential 8™ medium (Gibco) on Matrigel (BD, Corning) without penicillin/streptomycin. Cells were differentiated in a monolayer toward cardiomyocytes as previously described [45]. In short, human ES cells were cultured in E8 until 60% confluent. Cells were then supplemented with 1% DMSO enriched E8 medium for 24 h. On D0, cells were put on BPEL medium supplemented with Activin A (20 ng/ml, R&D Systems), BMP4 (20 ng/ml, R&D Systems), and CHIR99021 (1.5 μ M, Axon Medchem). At D3, medium was changed to BPEL with XAV939 (5 μ M, Tocris), and on D6, BPEL without any supplements was used. BPEL medium: IMDM, no phenol red (Gibco) and F12 Ham's F12 nutrient Mix (Gibco) in a 1:1 ratio supplemented with 5% (v/v) PFHM-II (Gibco), 0.25% (w/v) BSA, 1% (v/v) Chemically Defined Lipid Concentrate (Gibco), 0.1% ITS-X (Gibco), 450 μ M α -MTG (Sigma), 2 mM GlutaMax, 50 μ g/ml L-ascorbic acid 2-phosphate (Sigma), and 0.25% penicillin/streptomycin (10,000 U/ml, Gibco).

Lentiviral constructs and transduction

Lentiviral plasmids harboring luciferase reporters of the *Per2* and *Bmal1* promoters were described previously and kindly provided by Prof. Dr. Liu [36,37,72]. Viral particles were concentrated via ultracentrifugation after three harvests in HEK293T cells. Cells were

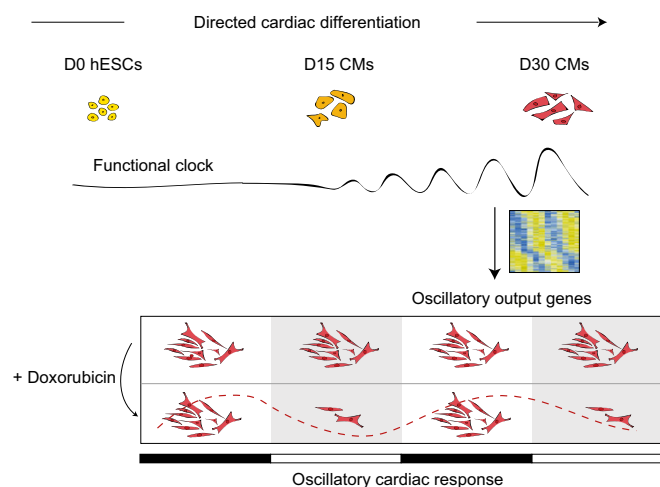


Figure 6. Schematic representation of the emergence and consequences of circadian rhythmicity during directed cardiac differentiation of human ES cells.

hESCs: human ES cells. CMs: cardiomyocytes.

transduced with concentrated Bmal1-dLuc or Per2-dLuc lentivirus 2 days before circadian bioluminescent measurements.

Bioluminescent recording and data analysis

Human ES cell-derived cardiac cells were differentiated for up to 45 days and transduced with lentiviral reporters at described time points after synchronization with 100 nM dexamethasone [47] for 2 h. Subsequently, medium was changed to recording medium [BPEL, 10 mM HEPES, 100 μ M D-Luciferin Potassium Salt (Promega)]. Human ES cells were cultured in E8 medium and synchronized for 2 h with forskolin [39]. Forskolin was chosen as a synchronizing agent for human ES cells, since dexamethasone has been implemented in multiple stem cell differentiation protocols and might therefore induce premature differentiation [73–78]. Subsequently, medium was changed to ES recording medium (E8, 10 mM HEPES, 100 μ M D-Luciferin Potassium Salt (Promega)). Culture dishes were sealed with high vacuum grease (Dow Corning) and monitored via the use of a LumiCycle32 device (Actimetrics) at 37°C. Bioluminescence from each dish was continuously recorded (integrated signal of 70 s with intervals of 10 min). Raw data (counts/s) were baseline subtracted (polynomial order 3).

Microscopic real-time bioluminescence analysis

Human ES cells were differentiated for up to 30 days and transduced with Bmal1-or Per2-dLuc lentivirus 2 days before recording. Bioluminescence was assessed with an LV200 microscope (Olympus) in a humidified chamber under 5% CO₂, at 37°C. Bioluminescence was detected for multiple consecutive days, using an EM CCD camera (Hamamatsu), with exposure times of 1 h. Image series were analyzed in ImageJ. Cells were synchronized with 100 nM dexamethasone for 2 h and changed to normal BPEL medium, containing 100 μ M D-Luciferin Potassium Salt (Promega). For pure cardiomyocyte population experiments, human ES cell-derived cardiac populations were sorted with a FACS Jazz flow cytometer (BD Biosciences) based on GFP positivity, replated on Matrigel-coated dishes, and bioluminescence was assessed 7 days later.

Immunostaining

Cells were fixed with 4% paraformaldehyde (PFA) for 15 min, blocked for 1 h in blocking buffer (5% FBS, 0.25% Triton X-100 in PBS), and stained for OCT4 (SantaCruz, #5279), NANOG (Cell Signaling, #3580S), TNNT2 (ThermoFisher Scientific, #MA5-12960), ACTN2 (Sigma, #A7811), MEF2C (Cell Signaling, #sc-13266), GFP (Abcam, #ab6556) in staining buffer (1% BSA, 0.25% Triton X-100 in PBS). Nuclei were stained with Hoechst for 15 min. Images were made using a spinning disk microscope (PerkinElmer).

RNA isolation and CEL-Seq

Cardiac cells were derived from human ES cells in 48-well plates. After synchronization, biological triplicates (independent wells) with comparable cardiac purity were collected every 4 h over the course of 48 h (ZT4-ZT48) (Fig EV3). RNA was extracted using the standard TRizol (Invitrogen) protocol, and 10 ng of total RNA per sample was used for library preparation and sequencing. RNA was

processed as described previously [49,79], and paired-end sequencing was performed on the Illumina Nextseq platform with a read length of 75 base pairs. Read 1 was used to identify the sample barcode and library index, while read 2 was aligned to the hg19 human RefSeq transcriptome (downloaded from the UCSC genome browser) using BWA [80]. CEL-Seq only sequences the most 3' end of a transcript, generating one read per transcript. Reads that mapped equally well to multiple locations were discarded. Around 500,000 reads were sequenced per sample. Samples were reads per million (RPM) normalized (Table EV1).

Quantitative RT-PCR

Purified RNA was treated with DNase (Promega) and reversibly transcribed with Superscript III reverse transcriptase (ThermoFisher Scientific). qRT-PCR on biological triplicate samples was carried out in triplicate (technical replicates) in CFX-384 Touch™ Real-time PCR detection system (Bio-Rad). *PPIA* was used as housekeeping gene, and fold changes were calculated to the lowest values among all replicates. Primer sequences: *PPIA* (fw): ttctgtctttgggacct, *PPIA* (rv): caccgtgtcttcgacattg, *NANOG* (fw): cagccctgattctc, *NANOG* (rv): tgcattctgctggaggctgag, *POU5F1* (fw): ctgaagcagaagagatg, *POU5F1* (rv): gggccgcagcttacacat, *ISL1* (fw): ctgcttttcagcaactggta, *ISL1* (rv): ggactggctaccatgctgtt, *NKX2-5* (fw): caagtgtgcctgcctttc, *NKX2-5* (rv): ctttctttcggctctagggtct, *ACTC1* (fw): atgcatcatgcctgctgat, *ACTC1* (rv): acgttcagcagtggtgacaa, *KCNJ2* (fw): tgggtcttgggaattctggttt, *KCNJ2* (rv): gaacatgtctctgttggcg, *SERCA2A* (fw): cgaaccttggcactcatct, *SERCA2A* (rv): ccagtattgcaggttcagggt, *BMAL1* (fw): ggctcatagatgcaaaaactgg, *BMAL1* (rv): ctccagaacataatc gagatgg, *PER2* (fw): ggccatccacaaaagatcctgc, *PER2* (rv): gaaaccga atgggagaatagtcg, *CRY1* (fw): ctccatggcactgttctcagtg, *CRY1* (rv): tccccaccaatttcagctgcaac, *CRY2* (fw): ccaagaggaagggcagggtagag, *CRY2* (rv): aggattgaggcactgttccagg, *CLOCK* (fw): aagttaggctgaaag acgacg, *CLOCK* (rv): gaactccgagaagaggcagaag, *NR1D1* (fw): acagctga caccaccagatc, *NR1D1* (rv): catgggcataggtgaagattct.

Western blotting

Cells were lysed in RIPA buffer, and protein concentration was measured using a BCA assay (ThermoFisher Scientific). 12.5 μ g protein lysate was loaded, separated by 10% SDS-PAGE, and transferred to a nitrocellulose membrane. Membranes were blocked with 5% milk powder (Nestlé) in T-BST and probed with anti-BMAL1 (1:1,000, #ab3350, Abcam), anti-CRY1 (1:1,000, #13474-1-A, Proteintech), or anti-CLOCK (1:250, #PA1-520, ThermoFisher Scientific) antibodies, followed by a peroxidase-conjugated antibody (1:5,000, #sc-2004, Santa Cruz). ECL Plus Western blotting substrate (#32132, ThermoFisher Scientific) was used for chemiluminescence detection with an ImageQuant™ LAS 4000 imager (GE Healthcare). HRP-coupled anti- β -ACTIN (1:5,000, #5125S, Cell Signaling) was used as a loading control. Band intensities were calculated with ImageJ.

Apoptosis measurements

Human ES cells were differentiated in 96-well white walled plates for the course of 15 and 30 days. Cardiac cells were synchronized with 100 nM of dexamethasone for 2 h, and 10 μ M of doxorubicin HCl (Sigma D1515) was administered at 6-h intervals for a total time

of 6 h. Apoptosis levels of three replicate wells (per condition), represented by active caspase 3 and caspase 7 levels, were measured using a CaspaseGlo 3/7 kit (Promega) following manufacturer's instructions. Bioluminescence was read out with a Centro microplate luminometer (Berthold Technologies).

JTK-cycle analysis

RPM-normalized read counts were obtained for each sample. As lowly expressed genes are typically not picked up robustly using CEL-Seq, genes with an average of > 3 RPM across all time points (ZT4-ZT48) as well as the replicates were selected for JTK-cycle analysis. Around 10,000 genes reached this threshold in both D15 and D30, and these form the list on which JTK-cycle was run (Table EV2). The following settings were used: *jtkdist* (12,3), periods (6:6), *jtk.init* (periods, 4). Significant oscillators with an adjusted *P*-value of < 0.05 were selected for further analyses. To identify mouse heart oscillators, JTK was run with similar settings on normalized GC-RMA intensity values of 24 samples (CT18-CT62, sampled every 2 h) for 35,556 genes downloaded from the GEO-database [81] (accession GSE54652) [14].

STRING and gene ontology analysis

STRING (Search Tool for the Retrieval of Interacting Genes/Proteins) database (www.string-db.org) was used to investigate the relationship between the overlap of known murine heart oscillators and identified D15 and D30 oscillators [56]. Gene ontology terms were retrieved via www.string-db.org.

CircaDB gene expression website

The circadian expression database (CircaDB, <http://circadb.hogenslab.org/>) is an open access online platform [59] compiling circadian gene expression profiles from microarrays and RNA sequencing experiments [11,14,18,82–88]. The embedded JTK-cycle algorithm defines the significance of rhythmic gene expression.

Statistics

All data were shown as means \pm s.e.m. Student's *t*-tests were carried out to assess differences between qRT-PCR mean values within the same experiments. One-way ANOVA, followed by a Bonferroni post hoc test, was carried out to test increasing mRNA levels of clock factors during directed cardiac differentiation. A difference of *P* < 0.05 was considered significant. To calculate general induction of apoptosis upon doxorubicin, a Mann-Whitney *U*-test was used. Differences in doxorubicin-effect sizes between D15 and D30 cardiac cells were assessed via non-overlapping 95% effect interval sizes. Statistical analyses to detect circadian oscillations in RNA levels (qRT-PCR) as well as doxorubicin-based apoptosis were performed by RAIN [40].

Data availability

Primary data

Dierickx P, Vermunt MW, Muraro MJ, Creyghton MP, Doevendans PA, van Oudenaarden A, Geijsen N, Van Laake LW (2017) Circadian

networks in human embryonic stem cell-derived cardiomyocytes. Gene Expression Omnibus GSE97142.

Referenced data

Zhang R, Lahens NF, Ballance HI, Hughes ME, Hogenesch JB (2014) A circadian gene expression atlas in mammals: Implications for biology and medicine. Gene Expression Omnibus GSE54652.

Expanded View for this article is available online.

Acknowledgements

We thank Prof. Dr. Christine Mummery, Dorien Ward-van Oostwaard (Leiden UMC) and Dr. David Elliot (Murdoch Childrens Research Institute) for providing us with the *NKX2-5*-eGFP human ES cell line, and Cathelijne W. van den Berg for the detailed differentiation protocol. We also thank Prof. Dr. Andrew Liu (University of Memphis) for sharing the lentiviral reporter plasmids. We thank Geert Geeven (Hubrecht Institute) for statistical assistance. This work was funded in part by NWO/ZonMw (Veni 91612147).

Author contributions

PD, PAD, LWVL, and NG conceived and designed the research; PD conducted and analyzed the experiments; MJM supervised by AvO, made sequencing libraries, and processed CEL-Seq data; PD and MWV supervised by MPC, analyzed and interpreted the CEL-Seq data; PD, MWV, NG, and LWVL wrote the paper.

Conflict of interest

The authors declare that they have no conflict of interest.

References

- Aschoff J (1983) Circadian control of body temperature. *J Therm Biol* 8: 143–147
- Ohishi K, Nagasato K, Aoi W, Nakamura T, Ichinose K, Nishiura Y, Satoh A, Tsujihata M, Shibata Y, Nagataki S (1993) Circadian rhythms of blood pressure and heart rate in patients with human T-lymphotropic virus type-I-associated myelopathy. *Tohoku J Exp Med* 169: 67–75
- Shea SA, Hilton MF, Hu K, Scheer FAJL (2011) Existence of an endogenous circadian blood pressure rhythm in humans that peaks in the evening. *Circ Res* 108: 980–984
- Richards AM, Nicholls MG, Espiner EA, Ikram H, Cullens M, Hinton D (1986) Diurnal patterns of blood pressure, heart rate and vasoactive hormones in normal man. *Clin Exp Hypertens A* 8: 153–166
- Degaute JP, Van Cauter E, van de Borne P, Linkowski P (1994) Twenty-four-hour blood pressure and heart rate profiles in humans. A twin study. *Hypertension* 23: 244–253
- Delp MD, Manning RO, Bruckner JV, Armstrong RB (1991) Distribution of cardiac output during diurnal changes of activity in rats. *Am J Physiol* 261: H1487–H1493
- Cajochen C, Kräuchi K, Wirz-Justice A (2003) Role of melatonin in the regulation of human circadian rhythms and sleep. *J Neuroendocrinol* 15: 432–437
- Pezuk P, Mohawk JA, Yoshikawa T, Sellix MT, Menaker M (2010) Circadian organization is governed by extra-SCN pacemakers. *J Biol Rhythms* 25: 432–441

9. Hara R, Wan K, Wakamatsu H, Aida R, Moriya T, Akiyama M, Shibata S (2001) Restricted feeding entrains liver clock without participation of the suprachiasmatic nucleus. *Genes Cells* 6: 269–278
10. Storch K-F, Lipan O, Leykin I, Viswanathan N, Davis FC, Wong WH, Weitz CJ (2002) Extensive and divergent circadian gene expression in liver and heart. *Nature* 417: 78–83
11. Tsimakouridze EV, Straume M, Podobed PS, Chin H, LaMarre J, Johnson R, Antenos M, Kirby GM, Mackay A, Huether P et al (2012) Chronomics of pressure overload-induced cardiac hypertrophy in mice reveals altered day/night gene expression and biomarkers of heart disease. *Chronobiol Int* 29: 810–821
12. Martino T, Arab S, Straume M, Belsham DD, Tata N, Cai F, Liu P, Trivieri M, Ralph M, Sole MJ (2004) Day/night rhythms in gene expression of the normal murine heart. *J Mol Med* 82: 256–264
13. Martino TA, Tata N, Belsham DD, Chalmers J, Straume M, Lee P, Pribiag H, Khaper N, Liu PP, Dawood F et al (2007) Disturbed diurnal rhythm alters gene expression and exacerbates cardiovascular disease with rescue by resynchronization. *Hypertension* 49: 1104–1113
14. Zhang R, Lahens NF, Ballance HI, Hughes ME, Hogenesch JB (2014) A circadian gene expression atlas in mammals: implications for biology and medicine. *Proc Natl Acad Sci USA* 111: 16219–16224
15. Eckel-Mahan K, Sassone-Corsi P (2013) Metabolism and the circadian clock converge. *Physiol Rev* 93: 107–135
16. Janich P, Toufighi K, Solanas G, Luis NM, Minkwitz S, Serrano L, Lehner B, Benitah SA (2013) Human epidermal stem cell function is regulated by circadian oscillations. *Cell Stem Cell* 13: 745–753
17. Janich P, Pascual G, Merlos-Suárez A, Batlle E, Ripperger J, Albrecht U, Cheng H-YM, Obrietan K, Di Croce L, Benitah SA (2011) The circadian molecular clock creates epidermal stem. *Nature* 480: 209–214
18. Rudic RD, McNamara P, Curtis A-M, Boston RC, Panda S, Hogenesch JB, FitzGerald GA (2004) BMAL1 and CLOCK, two essential components of the circadian clock, are involved in glucose homeostasis. *PLoS Biol* 2: e377
19. Kennaway DJ, Varcoe TJ, Voultsios A, Boden MJ (2013) Global loss of bmal1 expression alters adipose tissue hormones, gene expression and glucose metabolism. *PLoS ONE* 8: e65255
20. Bray MS, Ratcliffe WF, Grenett MH, Brewer RA, Gamble KL, Young ME (2013) Quantitative analysis of light-phase restricted feeding reveals metabolic dyssynchrony in mice. *Int J Obes* 37: 843–852
21. Furlan R, Barbic F, Piazza S, Tinelli M, Seghizzi P, Malliani A (2000) Modifications of cardiac autonomic profile associated with a shift schedule of work. *Circulation* 102: 1912–1916
22. Martino TA, Oudit GY, Herzenberg AM, Tata N, Koletar MM, Kabir GM, Belsham DD, Backx PH, Ralph MR, Sole MJ (2008) Circadian rhythm disorganization produces profound cardiovascular and renal disease in hamsters. *Am J Physiol Regul Integr Comp Physiol* 294: R1675–R1683
23. Penev PD, Kolker DE, Zee PC, Turek FW (1998) Chronic circadian desynchronization decreases the survival of animals with cardiomyopathic heart disease. *Am J Physiol* 275: H2334–H2337
24. Dierickx P, Du Pré B, Feyen DAM, Geijsen N, van Veen T, Doevendans PA, van Laake LW (2015) Circadian rhythms in stem cell biology and function. *Stem cells and cardiac regeneration*, pp 57–78. Cham: Springer International Publishing
25. Muller JE, Stone PH, Turi ZG, Rutherford JD, Czeisler CA, Parker C, Poole WK, Passamani E, Roberts R, Robertson T (1985) Circadian variation in the frequency of onset of acute myocardial infarction. *N Engl J Med* 313: 1315–1322
26. Mukamal KJ, Muller JE, Maclure M, Sherwood JB, Mittleman MA (2000) Increased risk of congestive heart failure among infarctions with nighttime onset. *Am Heart J* 140: 438–442
27. Tofler GH, Gebara OC, Mittleman MA, Taylor P, Siegel W, Venditti FJ, Rasmussen CA, Muller JE (1995) Morning peak in ventricular tachyarrhythmias detected by time of implantable cardioverter/defibrillator therapy. The CPI Investigators. *Circulation* 92: 1203–1208
28. Maron BJ, Semsarian C, Shen W-K, Link MS, Epstein AE, Estes NAM, Almquist A, Giudici MC, Haas TS, Hodges JS et al (2009) Circadian patterns in the occurrence of malignant ventricular tachyarrhythmias triggering defibrillator interventions in patients with hypertrophic cardiomyopathy. *Heart Rhythm* 6: 599–602
29. Arntz HR, Willich SN, Oeff M, Brüggemann T, Stern R, Heinzmann A, Matenaer B, Schröder R (1993) Circadian variation of sudden cardiac death reflects age-related variability in ventricular fibrillation. *Circulation* 88: 2284–2289
30. Maron BJ, Kogan J, Proschan MA, Hecht GM, Roberts WC (1994) Circadian variability in the occurrence of sudden cardiac death in patients with hypertrophic cardiomyopathy. *JAC* 23: 1405–1409
31. Durgan DJ, Pulinilkunnil T, Villegas-Montoya C, Garvey ME, Frangogiannis NG, Michael LH, Chow C-W, Dyck JRB, Young ME (2010) Short communication: ischemia/reperfusion tolerance is time-of-day-dependent: mediation by the cardiomyocyte circadian clock. *Circ Res* 106: 546–550
32. Reiter R, Swingen C, Moore L, Henry TD, Traverse JH (2012) Circadian dependence of infarct size and left ventricular function after ST elevation myocardial infarction. *Circ Res* 110: 105–110
33. Seneviratna A, Lim GH, Devi A, Carvalho LP, Chua T, Koh T-H, Tan H-C, Foo D, Tong K-L, Ong H-Y et al (2015) Circadian dependence of infarct size and acute heart failure in ST elevation myocardial infarction. *PLoS ONE* 10: e0128526
34. Suarez-Barrientos A, Lopez-Romero P, Vivas D, Castro-Ferreira F, Nunez-Gil I, Franco E, Ruiz-Mateos B, Garcia-Rubira JC, Fernandez-Ortiz A, Macaya C et al (2011) Circadian variations of infarct size in acute myocardial infarction. *Heart* 97: 970–976
35. Dierickx P, Doevendans PA, Geijsen N, van Laake LW (2012) Embryonic template-based generation and purification of pluripotent stem cell-derived cardiomyocytes for heart repair. *J Cardiovasc Trans Res* 5: 566–580
36. Liu AC, Welsh DK, Ko CH, Tran HG, Zhang EE, Priest AA, Buhr ED, Singer O, Meeker K, Verma IM et al (2007) Intercellular coupling confers robustness against mutations in the SCN circadian clock network. *Cell* 129: 605–616
37. Liu AC, Tran HG, Zhang EE, Priest AA, Welsh DK, Kay SA (2008) Redundant function of REV-ERB α and β and non-essential role for Bmal1 cycling in transcriptional regulation of intracellular circadian rhythms. *PLoS Genet* 4: e1000023
38. Umemura Y, Koike N, Matsumoto T, Yoo S-H, Chen Z, Yasuhara N, Takahashi JS, Yagita K (2014) Transcriptional program of Kpna2/Importin- α 2 regulates cellular differentiation-coupled circadian clock development in mammalian cells. *Proc Natl Acad Sci USA* 111: E5039–E5048
39. Yagita K, Okamura H (2000) Forskolin induces circadian gene expression of rPer1, rPer2 and dbp in mammalian rat-1 fibroblasts. *FEBS Lett* 465: 79–82
40. Thaben PF, Westermark PO (2014) Detecting rhythms in time series with RAIN. *J Biol Rhythms* 29: 391–400
41. Keller G (2005) Embryonic stem cell differentiation: emergence of a new era in biology and medicine. *Genes Dev* 19: 1129–1155

42. Elliott DA, Braam SR, Koutsis K, Ng ES, Jenny R, Lagerqvist EL, Biben C, Hatzistavrou T, Hirst CE, Yu QC et al (2011) NKX2-5(eGFP/w) hESCs for isolation of human cardiac progenitors and cardiomyocytes. *Nat Methods* 8: 1037–1040
43. Bunda S, Liu P, Wang Y, Liu K, Hinek A (2007) Aldosterone induces elastin production in cardiac fibroblasts through activation of insulin-like growth factor-I receptors in a mineralocorticoid receptor-independent manner. *Am J Pathol* 171: 809–819
44. Cao N, Huang Y, Zheng J, Spencer CI, Zhang Y, Fu J-D, Nie B, Xie M, Zhang M, Wang H et al (2016) Conversion of human fibroblasts into functional cardiomyocytes by small molecules. *Science* 352: 1216–1220
45. van den Berg CW, Elliott DA, Braam SR, Mummery CL, Davis RP (2015) Differentiation of human pluripotent stem cells to cardiomyocytes under defined conditions. *Methods Mol Biol* 1353: 163–180
46. Liu J, Lieu DK, Siu C-W, Fu J-D, Tse H-F, Li RA (2009) Facilitated maturation of Ca²⁺ handling properties of human embryonic stem cell-derived cardiomyocytes by calsequestrin expression. *Am J Physiol Cell Physiol* 297: C152–C159
47. Balsalobre A, Brown SA, Marcacci L, Tronche F, Kellendonk C, Reichardt HM, Schütz G, Schibler U (2000) Resetting of circadian time in peripheral tissues by glucocorticoid signaling. *Science* 289: 2344–2347
48. Yagita K, Horie K, Koinuma S, Nakamura W, Yamanaka I, Urasaki A, Shigeyoshi Y, Kawakami K, Shimada S, Takeda J et al (2010) Development of the circadian oscillator during differentiation of mouse embryonic stem cells *in vitro*. *Proc Natl Acad Sci USA* 107: 3846–3851
49. Hashimshony T, Wagner F, Sher N, Yanai I (2012) CEL-seq: single-cell RNA-seq by multiplexed linear amplification. *Cell Rep* 2: 666–673
50. Hughes ME, Hogenesch JB, Kornacker K (2010) JTK_CYCLE: an efficient nonparametric algorithm for detecting rhythmic components in genome-scale data sets. *J Biol Rhythms* 25: 372–380
51. Li J, Grant GR, Hogenesch JB, Hughes ME (2015) Considerations for RNA-seq analysis of circadian rhythms. *Meth Enzymol* 551: 349–367
52. Bray MS, Shaw CA, Moore MWS, Garcia RAP, Zanutta MM, Durgan DJ, Jeong WJ, Tsai J-Y, Bugger H, Zhang D et al (2008) Disruption of the circadian clock within the cardiomyocyte influences myocardial contractile function, metabolism, and gene expression. *Am J Physiol-Heart C* 294: H1036–H1047
53. Sheikh-Hamad D, Bick R, Wu G-Y, Christensen BM, Razeghi P, Poin-dexter B, Taegtmeier H, Wamsley A, Padua R, Entman M et al (2003) Stanniocalcin-1 is a naturally occurring L-channel inhibitor in cardiomyocytes: relevance to human heart failure. *Am J Physiol-Heart C* 285: H442–H448
54. Li L, Weng Z, Yao C, Song Y, Ma T (2015) Aquaporin-1 deficiency protects against myocardial infarction by reducing both edema and apoptosis in mice. *Sci Rep* 5: 13807
55. Yan L, Wei X, Tang Q-Z, Feng J, Zhang Y, Liu C, Bian Z-Y, Zhang L-F, Chen M, Bai X et al (2011) Cardiac-specific mindin overexpression attenuates cardiac hypertrophy via blocking AKT/GSK3 β and TGF- β 1-Smad signalling. *Cardiovasc Res* 92: 85–94
56. Szklarczyk D, Franceschini A, Wyder S, Forslund K, Heller D, Huerta-Cepas J, Simonovic M, Roth A, Santos A, Tsafou KP et al (2015) STRING v10: protein-protein interaction networks, integrated over the tree of life. *Nucl Acids Res* 43: D447–D452
57. Radici L, Bianchi M, Crinelli R, Magnani M (2013) Ubiquitin C gene: structure, function, and transcriptional regulation. *Adv Biosci Biotechnol* 04: 1057–1062
58. Wu C, Orozco C, Boyer J, Leglise M, Goodale J, Batalov S, Hodge CL, Haase J, Janes J, Huss JW et al (2009) BioGPS: an extensible and customizable portal for querying and organizing gene annotation resources. *Genome Biol* 10: R130
59. Pizarro A, Hayer K, Lahens NF, Hogenesch JB (2013) CircaDB: a database of mammalian circadian gene expression profiles. *Nucl Acids Res* 41: D1009–D1013
60. MacLennan DH, Kranias EG (2003) Phospholamban: a crucial regulator of cardiac contractility. *Nat Rev Mol Cell Biol* 4: 566–577
61. Chen EY, Xu H, Gordonov S, Lim MP, Perkins MH, Ma'ayan A (2012) Expression2Kinases: mRNA profiling linked to multiple upstream regulatory layers. *Bioinformatics* 28: 105–111
62. Nunn C, Zou M-X, Sobiesiak AJ, Roy AA, Kirshenbaum LA, Chidiac P (2010) RGS2 inhibits beta-adrenergic receptor-induced cardiomyocyte hypertrophy. *Cell Signal* 22: 1231–1239
63. Motloch LJ, Hu J, Akar FG (2015) The mitochondrial translocator protein and arrhythmogenesis in ischemic heart disease. *Oxid Med Cell Longev* 2015: 234104
64. Muller JE, Tofler GH, Stone PH (1989) Circadian variation and triggers of onset of acute cardiovascular disease. *Circulation* 79: 733–743
65. Peckova M, Fahrenbruch CE, Cobb LA, Hallstrom AP (1998) Circadian variations in the occurrence of cardiac arrests: initial and repeat episodes. *Circulation* 98: 31–39
66. Lefrak EA, Pitha J, Rosenheim S, Gottlieb JA (1973) A clinicopathologic analysis of adriamycin cardiotoxicity. *Cancer* 32: 302–314
67. Benjamin RS, Chawla SP, Ewer MS (1988) Adriamycin cardiac toxicity—An assessment of approaches to cardiac monitoring and cardioprotection. In *Organ directed toxicities of anticancer drugs*, Hacker MP, Lazo JS, Tritton TR (eds), Boston, MA: Martinus Nijhoff Publishing. Proceedings of the First International Symposium on the Organ Directed Toxicities of Anticancer Drugs, Burlington, VT, June 4–6, 1987
68. Maillet A, Tan K, Chai X, Sadananda SN, Mehta A, Ooi J, Hayden MR, Pouladi MA, Ghosh S, Shim W et al (2016) Modeling doxorubicin-induced cardiotoxicity in human pluripotent stem cell derived-cardiomyocytes. *Sci Rep* 6: 25333
69. Burridge PW, Li YF, Matsa E, Wu H, Ong S-G, Sharma A, Holmström A, Chang AC, Coronado MJ, Ebert AD et al (2016) Human induced pluripotent stem cell-derived cardiomyocytes recapitulate the predilection of breast cancer patients to doxorubicin-induced cardiotoxicity. *Nat Med* 22: 547–556
70. Guenther CJ, Luitje ME, Pyle LA, Molyneux PC, Yu JK, Li AS, Leise TL, Harrington ME (2014) Circadian rhythms of Per2: Luc in individual primary mouse hepatocytes and cultures. *PLoS ONE* 9: e87573
71. Reubinoff BE, Pera MF, Fong CY, Trounson A, Bongso A (2000) Embryonic stem cell lines from human blastocysts: somatic differentiation *in vitro*. *Nat Biotechnol* 18: 399–404
72. Ramanathan C, Khan SK, Kathale ND, Xu H, Liu AC (2012) Monitoring cell-autonomous circadian clock rhythms of gene expression using luciferase bioluminescence reporters. *J Vis Exp* 67: e4234
73. Cai J, Zhao Y, Liu Y, Ye F, Song Z, Qin H, Meng S, Chen Y, Zhou R, Song X et al (2007) Directed differentiation of human embryonic stem cells into functional hepatic cells. *Hepatology* 45: 1229–1239
74. Tropel P, Noël D, Platel N, Legrand P, Benabid A-L, Berger F (2004) Isolation and characterisation of mesenchymal stem cells from adult mouse bone marrow. *Exp Cell Res* 295: 395–406
75. Kubo A, Shinozaki K, Shannon JM, Kouskoff V, Kennedy M, Woo S, Fehling HJ, Keller G (2004) Development of definitive endoderm from embryonic stem cells in culture. *Development* 131: 1651–1662
76. Jaiswal N, Haynesworth SE, Caplan AI, Bruder SP (1997) Osteogenic differentiation of purified, culture-expanded human mesenchymal stem cells *in vitro*. *J Cell Biochem* 64: 295–312

77. Mackay AM, Beck SC, Murphy JM, Barry FP, Chichester CO, Pittenger MF (1998) Chondrogenic differentiation of cultured human mesenchymal stem cells from marrow. *Tissue Eng* 4: 415–428
78. Pittenger MF, Mackay AM, Beck SC, Jaiswal RK, Douglas R, Mosca JD, Moorman MA, Simonetti DW, Craig S, Marshak DR (1999) Multilineage potential of adult human mesenchymal stem cells. *Science* 284: 143–147
79. Simmini S, Bialecka M, Huch M, Kester L, van de Wetering M, Sato T, Beck F, van Oudenaarden A, Clevers H, Deschamps J (2014) Transformation of intestinal stem cells into gastric stem cells on loss of transcription factor Cdx2. *Nat Commun* 5: 5728
80. Li H, Durbin R (2010) Fast and accurate long-read alignment with Burrows-Wheeler transform. *Bioinformatics* 26: 589–595
81. Barrett T, Wilhite SE, Ledoux P, Evangelista C, Kim IF, Tomashevsky M, Marshall KA, Phillippy KH, Sherman PM, Holko M et al (2013) NCBI GEO: archive for functional genomics data sets—update. *Nucl Acids Res* 41: D991–D995
82. Hughes ME, DiTacchio L, Hayes KR, Vollmers C, Pulivarthy S, Baggs JE, Panda S, Hogenesch JB (2009) Harmonics of circadian gene transcription in mammals. *PLoS Genet* 5: e1000442
83. Miller BH, McDearmon EL, Panda S, Hayes KR, Zhang J, Andrews JL, Antoch MP, Walker JR, Esser KA, Hogenesch JB et al (2007) Circadian and CLOCK-controlled regulation of the mouse transcriptome and cell proliferation. *Proc Natl Acad Sci USA* 104: 3342–3347
84. Andrews JL, Zhang X, McCarthy JJ, McDearmon EL, Hornberger TA, Russell B, Campbell KS, Arbogast S, Reid MB, Walker JR et al (2010) CLOCK and BMAL1 regulate MyoD and are necessary for maintenance of skeletal muscle phenotype and function. *Proc Natl Acad Sci USA* 107: 19090–19095
85. Panda S, Antoch MP, Miller BH, Su AI, Schook AB, Straume M, Schultz PG, Kay SA, Takahashi JS, Hogenesch JB (2002) Coordinated transcription of key pathways in the mouse by the circadian clock. *Cell* 109: 307–320
86. Rudic RD, McNamara P, Reilly D, Grosser T, Curtis A-M, Price TS, Panda S, Hogenesch JB, FitzGerald GA (2005) Bioinformatic analysis of circadian gene oscillation in mouse aorta. *Circulation* 112: 2716–2724
87. Hoogerwerf WA, Sinha M, Conesa A, Luxon BA, Shahinian VB, Cornélissen G, Halberg F, Bostwick J, Timm J, Cassone VM (2008) Transcriptional profiling of mRNA expression in the mouse distal colon. *Gastroenterology* 135: 2019–2029
88. Keller M, Mazuch J, Abraham U, Eom GD, Herzog ED, Volk H-D, Kramer A, Maier B (2009) A circadian clock in macrophages controls inflammatory immune responses. *Proc Natl Acad Sci USA* 106: 21407–21412



License: This is an open access article under the terms of the Creative Commons Attribution-NonCommercial-NoDerivs 4.0 License, which permits use and distribution in any medium, provided the original work is properly cited, the use is non-commercial and no modifications or adaptations are made.